Analytica Chimica Acta 1231 (2022) 340436

Contents lists available at ScienceDirect

Analytica Chimica Acta

journal homepage: www.elsevier.com/locate/aca

Sequence-specific amperometric detection based on a double-probe mode and enzyme-mediated multiple signal electrocatalysis for the double-stranded DNA of PML/RARα-related fusion gene

Yun Lei [a], Kun Wang [a,b], Jia-Yong Yang [b], Xin-Hua Lin [a,**], Ai-Lin Liu [a,*]

[a] Department of Pharmaceutical Analysis, Higher Educational Key Laboratory for Nano Biomedical Technology of Fujian Province, The School of Pharmacy, Fujian Medical University, Fuzhou, 350122, China
[b] The First Affiliated Hospital of Xiamen University, Xiamen, 361003, China

HIGHLIGHTS

- An E-DNA biosensor based on dual-probe mode and enzyme-mediated multiple signal electrocatalysis is constructed.
- The dual-probe E-DNA biosensor exhibits excellent selectivity and specificity for detection of a larger dsDNA segment.
- The practicability of this biosensor is well proven by determining both PCR products and enzyme-digested PCR products.
- The dual-probe biosensor provides an alternative method for the development of rapid and sensitive diagnostic platform.

GRAPHICAL ABSTRACT

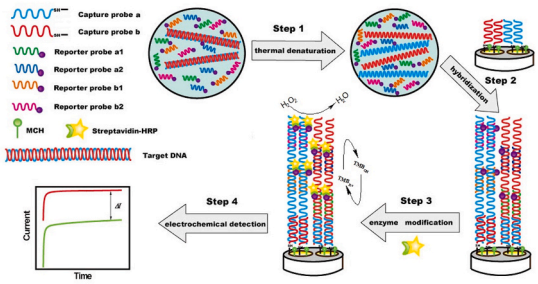

ARTICLE INFO

Keywords:
Electrochemical DNA biosensor
Dual-probe detection model
Signal amplification
PML/RARα fusion gene
Large double-stranded DNA fragment

ABSTRACT

A new electrochemical DNA biosensor based on double-probe mode and enzyme-mediated multiple signal electrocatalysis is constructed for the highly sensitive determination of double-stranded (ds-) PML/RARα fusion gene. Through the ingenious design of two groups of detection probes, including two thiolated capture probes anchored on dual standalone detection units integrated into one customized gold electrode and four biotinylated reporter probes, hybridizing with different segments of the same target single-stranded DNA (ssDNA) simultaneously, the hybridization efficiency between the probes and target is improved by preventing the reannealing of the two separate target ssDNA. Compared with a single reporter probe, this method can dramatically increase the amount of biotin and introduce numerous streptavidin-labelled horseradish peroxidase (HRP), thereby significantly amplifying electrochemical signals with low background signals. The combination of the dual-probe mode, multiple signal amplification strategy, and the inherent electrocatalytic activity of the HRP results in the prominent electrochemical sensing performance in detecting large-fragment target dsDNA with a detection limit as low as 71 fM. Furthermore, taking advantage of the new detection strategy, polymerase chain reaction

* Corresponding author.
** Corresponding author.
E-mail addresses: xhl1963@sina.com (X.-H. Lin), ailinliu@mail.fjmu.edu.cn (A.-L. Liu).

https://doi.org/10.1016/j.aca.2022.340436
Received 28 April 2022; Received in revised form 22 August 2022; Accepted 21 September 2022
Available online 27 September 2022

(PCR) products and enzyme-digested PCR products from NB4 cells can be effectively analysed, showing great promise for the development of a new class of point-of-care platforms for disease-/drug-related genes.

1. Introduction

Acute promyelocytic leukemia (APL) is the designated M3 type of acute myelogenous leukemia (AML) in the French – American – British (FAB) classification. It is characterized by a specific chromosomal translocation t (15; 17), promyelocytic leukemia/retinoic acid receptor alpha (PML/RARα) fusion gene generation, and the repressive effects of the encoded fusion protein on myeloid differentiation [1–4]. If APL cannot be diagnosed and treated timely, it often combines with the concurrent diffuse intravascular coagulation (DIC) and primary fibrinolysis, which causes severe bleeding, and even death. Thus, the early diagnosis and long-term monitoring of minimal residual disease for APL are important. Importantly, arsenic trioxide (ATO) and/or all-transretinoic acid (ATRA), which function as repressors in super-enhancer-associated PML/RARα-regulated targets, are widely used in APL therapy [5]. Thus, the PML/RARα, as a distinct marker gene in APL, plays a vital role in the diagnosis and treatment of APL [6–9].

Electrochemical deoxyribonucleic acid (DNA) biosensors (E-DNA biosensors) are analytical devices for nucleic acid sensing by the hybridization of specific target sequences with complementary probes immobilized on the surface of a substrate. The E-DNA biosensors show great promise as devices fit for point-of-care testing (POCT) and multiplexing platforms for the analysis of nucleic acids, with the merits of high sensitivity, fast response, integrated miniaturization, simple operation, low cost, etc. [10–15]. Over the past decade, our laboratory has conducted in-depth research on the employment of the E-DNA biosensors for PML/RARα fusion gene detection and has achieved some results [16–24]. First, we used a traditional DNA-sensing model, in which a single set of DNA probe molecules were modified on a single electrode to detect the target ssDNA. A series of genosensors have been developed by introducing different functional materials (e.g., polymer, hydrogel, and metal nanomaterial) [16–18] and new-style detection probes (e.g., hairpin probe and locked nucleic acids) [19,20] for good sensitivity and specificity in the DNA detection. These proposed methods perform well in the detection of short synthetic single-stranded segments, while they perform poorly when dealing with biological DNA samples. Such a problem occurred because, first, most of the target DNA fragments derived from biological samples are in the form of native double-stranded (ds-) segments, leading to the loss of the hybridization efficiency between the short DNA probes and the target sequences. Second, despite having been unstranded before detection, the reannealing of two separate ssDNA from the target dsDNA could seriously hinder heterogeneous hybridization on the electrode surface. Finally, some reported E-DNA biosensors integrated with the asymmetric polymerase chain reaction (PCR) technique enable the production of numerous target ssDNA amplicons and the direct detection of the targets [25–27]. However, those demonstrations are not satisfactory because of the low efficiency of the asymmetric PCR and requirement of the complex optimization of primer concentrations [28,29].

Considering the above predicament for the design of a sensitive E-DNA system for real applications, one key point should be emphasised: how to simultaneously improve the hybridization efficiency between the probe and dsDNA and hold back the reannealing of the two separate ssDNA to achieve the direct detection of the dsDNA in actual clinical samples. Therefore, our group has adopted the interfering probes in the hybridization solutions to prevent the reannealing of the original dsDNA with satisfactory results in double-stranded PCR amplicon assaying [22]. Inspired by this observation, we proposed a novel dual-probe detection model containing two sets of DNA probes modified on the surface of the two working electrodes (dual-channel electrodes) for detecting two complementary strands from the target dsDNA [23,24]. Both dual-probe detection approaches have achieved outstanding detection specificity and sensitivity in detecting synthetic dsDNA fragments. We credit this superiority to the use of a specific probe design ("*Y*" junction structure probe and oligonucleotide analog) and restriction endonuclease-assisted cyclic enzymatic amplification strategy. For this step, the synthetic target dsDNA involved are short-length sequences (22 bp and 60 bp). Upon hybridization with a large segment from biological samples, the sensitivity is limited because the remnant sequence chain is prone to fold and curl, leading to an inevitable steric effect on the heterogeneous surface and the attenuated hybridization efficiency of the probes and target. In addition, the new-style detection probes increase the experimental cost, and the induced endonuclease generates a high blank signal. Further, the current signals of the dual-channel electrodes can be collected only using a dual-channel electrochemical device, which is unfavourable for developing simplified protocols.

In this study, aiming to develop advanced electrochemical biosensors better suited to miniaturization and integration for POCT devices, we design a high-performance dual-probe detection model with remarkable improvements in sensitivity and selectivity towards large target dsDNA. Further, we simplify the instrumentation using a previously reported dual-channel sandwich structure detection method and a multiple signal amplification strategy. The dual-probe detection signals are collected from two independent detection units of the tailored gold electrode (d-AuE), which is achieved using a traditional single-channel electrochemical device with a relatively simple connection circuit. Given the large size and double-stranded existence form of the target dsDNA in biological samples, the E-DNA biosensor involved two pairs of detection probes, consisting of two thiolated capture probes (Ca/Cb) immobilized on two separated surfaces of d-AuE and four biotinylated reporter probes (Ra1, Ra2, Rb1, and Rb2). The main aim of this strategy is to hinder the reannealing of the two specific strands from the target dsDNA by designing the complementary position of the reporter probes and to increase the overall detection current signals through increasing the amount of biotins functionalized on the surface of the d-AuE. The proposed method is evaluated and used to determine the PCR products and enzyme-digested PCR products of the PML/RARα fusion gene from the NB4 cell.

2. Materials and Methods

The details of the "Materials and Methods" section are shown in the Supporting Information.

3. Results and discussion

3.1. The principles of the dual-probe E-DNA biosensor based on enzyme-mediated multiple signal electrocatalysis

The principle of the E-DNA biosensor based on dual-probe mode and enzyme-mediated multiple signal amplification using d-AuE to determine the target dsDNA is depicted in Scheme 1. First, for the further miniaturization of the electrochemical device requiring two three-electrode systems in our previous studies, two round detection units (2 mm in diameter) with a distance of 2 mm were incorporated into the same gold working electrode (abbreviated as d-AuE). The integration of the working electrodes revealed some advantages of the relatively low sample volumes, relatively simple connection circuit, and excellent reliability of the signal output. Additionally, the dual-probe E-DNA biosensor involved two pairs of detection probes, that is, two thiolated capture probes (Ca and Cb) immobilized on two independent detection

units of d-AuE and four biotinylated reporter probes (Ra1, Ra2, Rb1, and Rb2), which are complementary to the interval parts of the corresponding target ssDNA. Of note, the number of biotinylated reporter probes increased from two to four for the inhibition of the reannealing of the two separate strands from the target dsDNA and the amplification of the overall detection current signals. Once the target dsDNA (S3a–S3b) appeared, the detection probes (Ca/Ra1Ra2 and Cb/Rb1Rb2) flanked the related complementary sequences after thermal denaturation. Further, the binding event afforded two sandwich-type dsDNA complexes (Ca/S3a/Ra1Ra2 and Cb/S3b/Rb1Rb2) on the dual detection zones of d-AuE. Thereafter, the biotin-modified dsDNA complexes introduced numerous streptavidin-labelled horseradish peroxidase (HRP), significantly increasing the electrochemical signals by the direct electrochemistry and electrocatalysis of HRP. Conversely, the biotinylated reporter probes were not captured onto the d-AuE surface without the target dsDNA, and thus, only very few streptavidin-HRP conjugates were tethered onto the electrode surface to catalyze a 3, 3′, 5, 5′-tetramethylbenzidine (TMB) substrate or amplify the signals. The target dsDNA could be detected by the variation of the current signals.

3.2. The feasibility study of the dual-probe E-DNA biosensor

Restriction endonucleases were employed to digest PCR products to generate the expected large fragment of the dsDNA. Well-chosen enzyme cut sites could influence the production of fragments with different lengths and sequences, and is fundamental for designing the detection probes and successfully constructing a more applicable detection protocol for the large fragment of the target dsDNA. Thus, the sites of restriction digested on the PCR product were analysed using Primer 5 software. By analyzing the position of the PML/RARα fusion site and the restriction enzyme site maps of the PCR-produced DNA sequence, a desirable restriction fragment with a length of 122 bp was obtained (Fig. S1) and used as the bio-recognition element. Meanwhile, the detection probes were designed according to the DNA sequences of the restriction fragment (shown in Supplemental Information, Table S2). The binding site of the fusion site located in the capture probe, while the reporter probes was complementary with the interval sequence of the same target ssDNA to considerably avoid the cross-interaction of the detection probes. For the specificity of the developed detection probes, two groups of the detection probes (Ca/Ra1Ra2 and Cb/Rb1Rb2) were designed based on the melting temperatures in the hybridization system according to the target dsDNA sequence. Further, the thermodynamic parameters of all oligonucleotides involved in the experiment were calculated using integrated DNA technologies (http://www.unafold.org/ [30], shown in Supplemental Information, Table S3). Moreover, the interface properties of the surface-modified d-AuE were severally investigated by cyclic voltammetry (CV) in 10 mM $K_3Fe(CN)_6$ solution and electrochemical impedance spectroscopy in a 10 mM $[Fe(CN)_6]^{3-/4-}$ solution containing 0.1 M KCl to reflect the preparation of the E-DNA biosensor (Fig. S2).

Furthermore, the electrochemical responses of the prepared biosensor were investigated to characterize the feasibility of the proposed strategy (Fig. 1). Fig. 1A compares the CV curves of different modified d-AuE in the TMB substrate. A prominent catalytic reduction peak was observed in the CV of the streptavidin-HRP modified d-AuE (HRP/Ra1Ra2S3a-Rb1Rb2S3b/MCH/Ca-Cb/d-AuE, Fig. 1A, curve b). Additionally, by comparing the current (*i*)–time (*t*) curves for the different modified d-AuE, the value of the amperometric current generated by catalysing the streptavidin-HRP was observed to be larger (1503 nA/mm^2, Fig. 1B, curve b) than that of the amperometric current without enzymatic catalysis (9 nA/mm^2, Fig. 1B, curve a). It turns out that upon hybridization, the streptavidin-HRP could conjugate with the two 'sandwich' structures containing four kinds of biotinylated reporter probes (Ca/S3a/Ra1Ra2 and Cb/S3b/Rb1Rb2) *via* affinity bond to be specifically modified onto the dual detection units of the d-AuE. However, if the 'sandwich' structures failed to be formed without the target dsDNA, few HRP could be fixed onto the d-AuE. The current strength, which was produced by the catalytic reduction of H_2O_2 with the redox reaction of TMB, significantly decreased. Therefore, the results indicated that the dual-probe E-DNA biosensor could significantly determine if the target dsDNA was in the solution under test using the TMB – HRP – H_2O_2 reaction system at the surface of the d-AuE. Additionally, we have reported that the PML/RARα dsDNA (fragment length, 60 bp) in the same concentration was detected using a commercial gold working electrode (AuE, 2 mm in diameter), and the average current signal intensity collected was 3260 nA [22], which was equivalent to the current density of 1038 nA/mm^2. In contrast, the current density (1503 nA/mm^2) of the PML/RARα dsDNA fragments (fragment length at approximately 122 bp) detected by the d-AuE in this work was 1.44 times higher than that of the above-mentioned report. In our previous research for detecting PML/RARa dsDNA short fragments (60 bp) using dual-channel electrodes, it was shown that the current signal intensities collected by two channels were 2700 nA (approximately equal to 859 nA/mm^2) and 2580 nA (approximately equal to 821 nA/mm^2) [24]. They were lower than those detected in this study. These results demonstrated that the subtle multiple reporter-probe design endowed the better sensitivity and specificity of the E-DNA biosensor even in the challenge with the large fragment of the PML/RARα dsDNA.

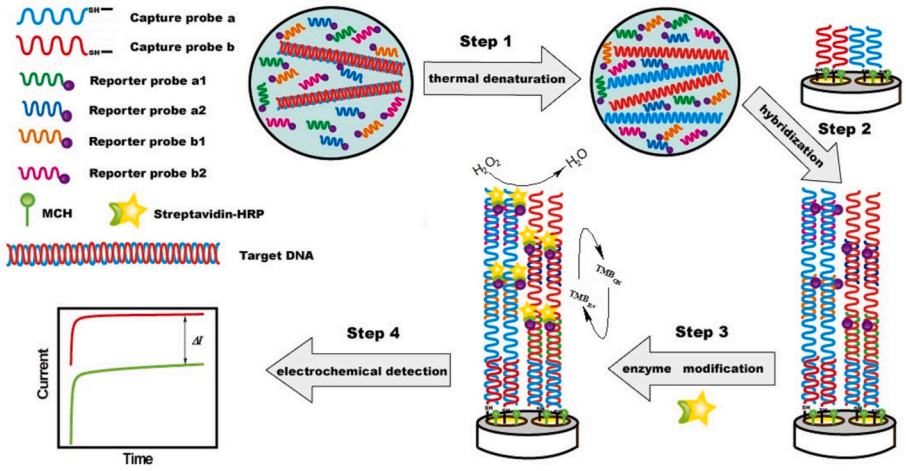

Scheme 1. Schematic diagram of the E-DNA biosensor based on dual-probe mode and enzyme-linked amplified multiple signals technology using d-AuE for detecting the PML/RARα fusion gene dsDNA.

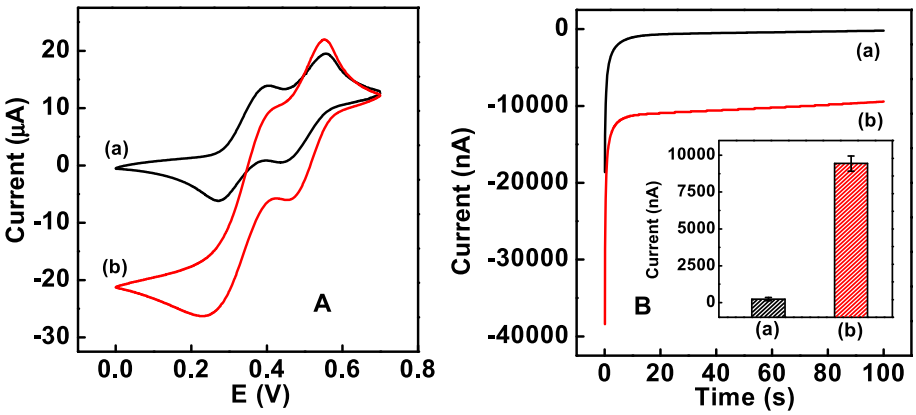

Fig. 1. Cyclic voltammograms (A) and current-time curves (B) of the TMB substrate at different modified customized d-AuE: (a) MCH/Ca-Cb/d-AuE; (b) HRP/Ra1Ra2S3a-Rb1Rb2S3b/MCH/Ca-Cb/d-AuE.

3.3. Optimization of the experimental conditions

The factors which could affect the analytical performance of the dual-probe E-DNA biosensor were investigated in details. To exclude co-interference between the factors, all experiments in this section were performed on commercial gold working electrodes (AuE, 2 mm in diameter), except for the optimization of the reporter probe concentrations which was performed on the d-AuE.

3.3.1. Investigation of the hybridization temperature

During the entire hybridization process, the temperature played a significant role in the specificity and efficiency of the hybridization. The melting temperature (T_m), as a physical property of nucleic acids, manifested the stability of duplexes in a specific milieu to validate the

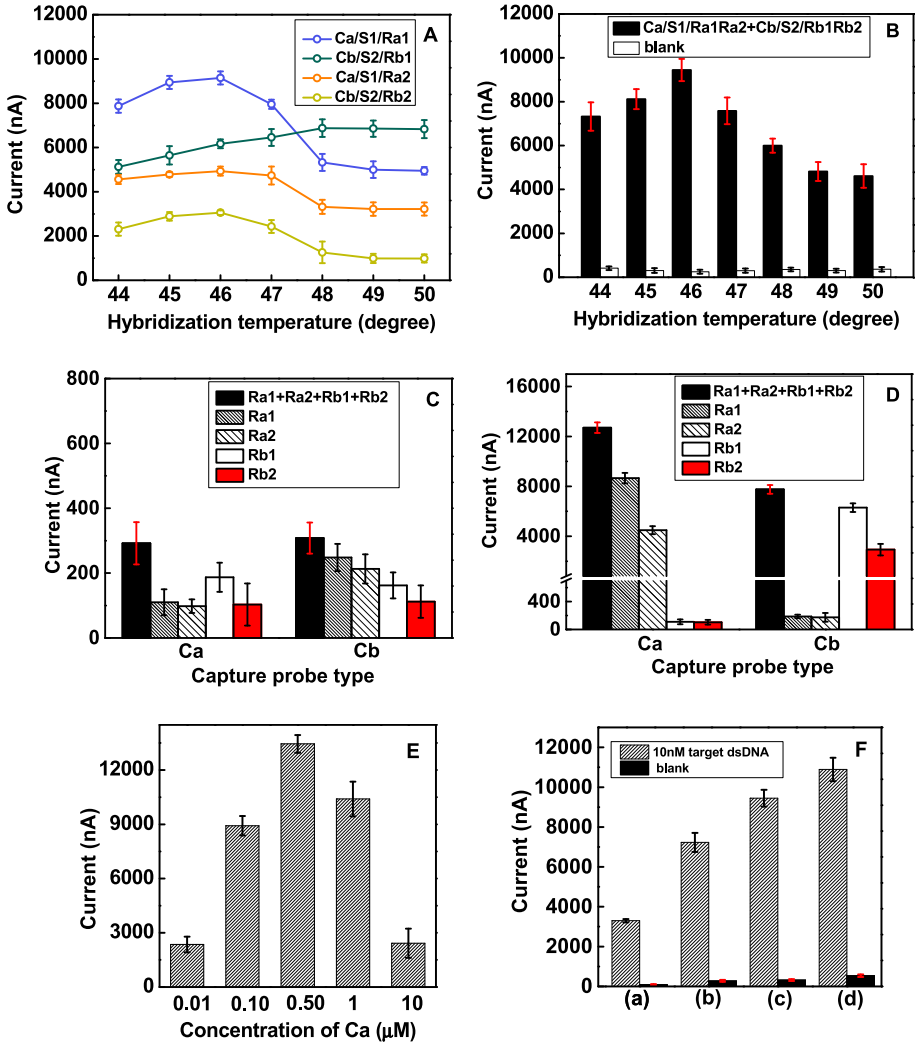

Fig. 2. (A) The relation graph between the temperatures and currents from the hybridization between different reporter probes and relevant complementary ssDNA using the single-capture-probe modified AuE. (B) Amperometric responses corresponding to different temperatures for detecting the target dsDNA using the dual-capture-probe modified d-AuE. (C) Amperometric responses of the hybridization between different capture probes and reporter probes (100 μM); (D) Amperometric responses of the hybridization of different capture probes, reporter probes (100 μM), and relevant complementary ssDNA (10 nM). (E) Comparison of current responses of the hybridization with target ssDNA S1 (10 nM) and reporter probes (Ra1+Ra2) on the AuE modified with different assembly concentrations of the capture probe (Ca, 0.01, 0.10, 0.50, 1, and 10 μM). (F) Comparison of the detection of the target dsDNA (S3, 10 nM) by equal amounts of the reporter probes (Ra1+Ra2+Rb1+Rb2) with different concentrations: (a) 10 nM; (b) 50 nM; (c) 100 nM; (d) 500 nM.

nucleic acid probes available for the special recognition of complementary sequences. According to the above-mentioned values of T_m calculated by the integrated DNA technologies (Table S3), the hybridization temperature was further studied in the range from 44 °C to 50 °C by amperometric measurement. Given the reannealing interference from two separate strands from the target duplexes during the testing process, the current signals of the hybridization between the target ssDNA (S1 or S2) with the matching capture probe (Ca or Cb) and single reporter probe (Ra1, Ra2, Rb1 or Rb2) were studied under different hybridization temperatures. The study comprised four hybridization systems of the probes/target duplexes, i.e. Ca/S_1/Ra1, Ca/S1/Ra2, Cb/S2/Rb1, and Cb/S2/Rb2.

According to the results (Fig. 2A), we observed that the current responses increased with the increase in hybridization temperature and levelled off above 46 °C in the three hybridization systems (Ca/S1/Ra1, Ca/S1/Ra2, and Cb/S2/Rb2). This might be because the increasing thermal motion of the molecule under the relatively high temperature unwound the dsDNA formed by hybridization. For Cb/S2/Rb1, the strongest current signal appeared at 48 °C. Similarly, the detection signal declined with the increase in temperature due to the enhancement of thermal motion. The best hybridization temperatures for the different detection probes were somewhat different. Additionally, we noted that the ranking order of the current intensity for these hybridization systems was as follows: Ra1 > Rb1 > Ra2 > Rb2. This observation was relative to the distances between the streptavidin-HRP captured by the biotinylated reporter probes and the d-AuE surface. In the proposed multiple signal amplification strategy, we designed dual reporter probes to be complementary to different segments of the same target ssDNA. As shown in Scheme 1, the hybridization of Ra1 with the complementary strand from the target dsDNA occurred close to the d-AuE, while the hybridization of Ra2 occurred in far proximity. In general, the shorter the distance between the enzyme and the electrode surface, the faster the electron transfer on the electrode surface and the larger the current signal. Such a trend of current response validated the hypothesis about the location of four reporter probes on the two sandwich DNA structures, demonstrating the likelihood of the successful assembly of the expected E-DNA biosensor.

On the basis of the above result, the influence of the reaction temperature on the target dsDNA detection using the dual-probe E-DNA biosensor was investigated further. Fig. 2B shows the current signals corresponding to different temperatures (ranging from 44 °C to 50 °C) for detecting 10 nM target dsDNA (S3a-S3b) by amperometric measurements. As displayed in Fig. 2B, the maximum value of the current signal appeared at 46 °C (9440 nA), where the hybridization efficiency of the detection probes is the highest. The current signal at relatively low temperatures (44 °C and 45 °C) was 77%–85% of the maximum value at 46 °C. Conversely, increasing the hybridization temperature (>46 °C) causes a notable decline in current signal below 50%, ascribed to the accelerating denaturation of the detection probes/target DNA complexes (Ca/S3a/Ra1Ra2 and Cb/S3b/Rb1Rb2) and the decreasing hybridization number. Furthermore, the detected signals of the hybridization background (namely the hybridization system without target dsDNA) remained at a nearly constant low value at all reaction temperatures. Taken together, 46 °C was selected as the optimized hybridization temperature during the whole experimentation.

3.3.2. Optimization of detection probes

The specificity of the designed detection probes was initially investigated because of the coexistence of many detection probes in the hybridization system (shown in Fig. 2C). According to the results, the detected hybridization current signals from the different combinations of the capture probes (Ca or Cb) and reporter probes (Ra1, Ra2, Rb1, Rb2 or Ra1/Ra2/Rb1/Rb2) were all under 350 nA. This indicated that there were few hybridization reactions between the detection probes.

Furthermore, taking into account that multiple hybridization reactions among different DNA segments might occur simultaneously, we investigated the identification ability of the detection probe to the corresponding target ssDNA (S_1 or S_2) in the above-mentioned hybridization systems (shown in Fig. 2D). The results indicate that the combination detection probes (Ca/Ra1 and Ca/Ra2) could simultaneously recognise the corresponding segments of S1 under the same condition. However, no hybridization reaction was observed between S1 and the combination detection probes (Ca/Rb1 and Ca/Rb2) because of the mismatch between the reporter probe (Rb1 or Rb2) and S1. Similarly, the combination detection probes (Cb/Rb1 and Cb/Rb2) presented the specific identification of the complementary sequence of S2. Additionally, we employed the combination detection probes (Ca/Ra1+Ra2+Rb1+Rb2 and Cb/Ra1+Ra2+Rb1+Rb2) to analyse the corresponding target ssDNA (S_1 and S_2, respectively). The current signals of the combination detection probes containing mixed reporter probes (Ca/Ra1+Ra2+Rb1+Rb2 and Cb/Ra1+Ra2+Rb1+Rb2) were stronger than those of the combination detection probes that contained one single reporter probe (Ca/Ra1, Ca/Ra2, Cb/Rb1, and Cb/Rb2). That was because the increasing number of biotinylated reporter probes amplified the payload of the streptavidin-HRP, sharply enhancing the amperometric signal of the TMB–HRP–H_2O_2 system. These results demonstrated that the designed detection probes possessed a superior recognition ability towards the complementary target strand and effectively suppressed nonspecific current signals from the cross-hybridization of these probes.

During the construction of the E-DNA biosensor, the immobilization of the capture probes (Ca and Cb) on the electrode surface was a vital step because the capture probe and the two corresponding biotinylated reporter probes (Ca/Ra1Ra2 and Cb/Rb1Rb2) simultaneously flanked different segments of the same complementary target. Afterwards, the streptavidin-HRP was specifically captured *via* biotin–streptavidin binding, which could be limited by steric hindrance. Therefore, the density of the capture probes directly affected the payload of the anchored streptavidin–HRP molecule and the performance of the sensor. Using Ca/Ra1Ra2 as an example, different assembled concentrations of Ca were investigated (0.01, 0.10, 0.50, 1, and 10 μM) on the AuE. As shown in Fig. 2E, the current signal saw a fast growth with the augment of the capture probe Ca concentration from 0.01 to 0.50 μM because of the increased number of detection probes/target hybrids produced. Thereafter, a decrease in the current intensity was observed when the concentration was higher than 0.50 μM, suggesting that a high-density capture probe monolayer reduced the hybridization efficiency of the probes with the target strand and strengthened the steric hindrance of the enzyme. Therefore, 0.50 μM was selected as the optimal assembly concentration of the capture probes with optimized molecular distance for the HRP enzyme.

Additionally, the concentrations of these reporter probes (Ra1, Rb1, Ra2, and Rb2) added to the hybridization system had a specific influence on the performance of the dual-probe E-DNA biosensor. Therefore, we optimized the content of the four reporter probes with identical concentrations in the hybridization solution in the experiment (shown in Table S4). As shown in Fig. 2F, with the increase in the concentration of each reporter probe (from 10 nM to 500 nM) in the hybridization solution, the values of the current signals increased. This phenomenon demonstrated that more reporter probes would efficiently hinder the reannealing of the two separate strands from the target dsDNA, thereby improving the hybridization probability between the reporter probes and target dsDNA. However, we noted that the current signal of the background was exacerbated. According to the above experimental results, 100 nM was selected in the following experiments to ensure the high hybridization efficiency and signal-to-noise ratio.

3.4. Study on the specificity and sensitivity of the dual-probe E-DNA biosensor for dsDNA detection

It is important to determine a method to ensure the high recognition ability between the dual detection probes and target dsDNA for the dual-

probe E-DNA biosensor based on enzyme-mediated multiple signal electrocatalysis for signal amplification. Thus, we investigated the specificity of our E-DNA biosensor *via* detecting a series of different dsDNA sequences (see Table S1 for details), including the fully complementary target dsDNA (S3), five-base mismatch dsDNA (S4), ten-base mismatch dsDNA (S5), PML partial dsDNA (S6), and RARα partial dsDNA (S7). The amperometric technique, providing a rapid and direct measurement of the current related to the HRP electrocatalytic process, was employed to detect these dsDNA fragments in the hybridization solution in turn. As shown in Fig. 3A, compared with the blank signal, only complementary dsDNA (S3) caused a strong current response, whereas negligible signals were observed when the number of mismatch bases was greater than or equal to 5 (S4, S5, S6, and S7) since no effective hybridization occurred. This result indicated that the detection probes exhibited an outstanding discriminatory capacity and held promise for the detection of complex clinical samples.

The analytical performance of the dual-probe E-DNA biosensor toward the complementary target dsDNA at a series of concentrations was assessed in a phosphate-buffered saline (PBS) hybridization solution (Fig. 3B). The E-DNA biosensor was challenged with the target dsDNA across the range of 100 fM–10 nM, spanning a response region of 5 orders of magnitude (Fig. 3C). Significantly, the detection performance of the dual-probe detection mode used for the dsDNA detection surpassed the counterpart based on the single group of detection probes (Ca/Ra1Ra2: dense or Cb/Rb1Rb2: white in Fig. 3C) at every concentration point. Under the optimal hybridization condition, the current signal was aggrandised with the increase in the concentration of the target ranging from 0.50 pM to 50 pM. Further, good linearity was observed between the signal responses and the logarithmic function of the target dsDNA concentration, with a limit of detection (LOD) as low as 71 fM (the inset in Fig. 3C). As previously reported by our lab, for instance, the E-DNA biosensor can be implemented to detect the target dsDNA (60 bp) within the concentration range of 0.50–10 nM and a LOD of 1 pM [22]. And another reported dual-channel electrode showed that the complementary DNA concentration range of the target dsDNA was from 50 pM to 5 nM with a LOD of 9.20 pM [24]. Additionally, the assay precision of the E-DNA biosensor was evaluated using five different modified d-AuE fabricated independently. The relative standard derivation (RSD) of current response for 10 nM target dsDNA was 9.8%, indicating acceptable precision and reproducibility of the biosensor. Thus, compared with the results of previous reports, the present study exhibited prominent detection performance towards the quantitative detection of a relatively large dsDNA segment.

3.5. Detection of the PCR products and enzyme-digested PCR-amplified products from clinical samples

To challenge the practicability of our dual-probe E-DNA biosensor, we analysed the PCR products and enzyme-digested PCR products from the NB4 cell supplied by the Fujian Institute of Hematology. In a preliminary evaluation study for APL detection, we studied the detection performance of the biosensor for PCR products and enzyme-digested PCR amplified products. The PCR was amplified using DNA extracted from the NB4 cell as a template, and the PCR products were digested using two restriction enzymes. Subsequently, two kinds of products were verified by 1.5% agarose gel electrophoresis (Fig. 4A). Additionally, the PCR products from the K562 cell, human chronic myeloid leukemia cell line, were chosen as the negative control. The PCR amplification products (lane 2) and enzyme-digested PCR products (lane 3) from the NB4 cell showed characteristic bands of the expected sizes (approximately 151 bp and 122 bp, respectively), while an inconspicuous band was observed in the negative PCR samples (lane 4).

To determine if the PCR-positive product harboured the targeted gene segment, the PCR product from a positive real sample was determined to obtain an accurate sequence by gene sequencing. From the partial output data (Fig. 4B), we observed that the PCR-positive product was a 151-bp targeted fragment, which contained a PML/RARα fusion site. Furthermore, according to the restriction enzyme cutting sites and the related restriction enzymes of the PML/RARα fusion gene partial sequence (shown in Fig. S1), it can be speculated that the enzyme-digested PCR products contained the corresponding target sequence with a length of 122 bp. We applied the dual-probe E-DNA biosensor to

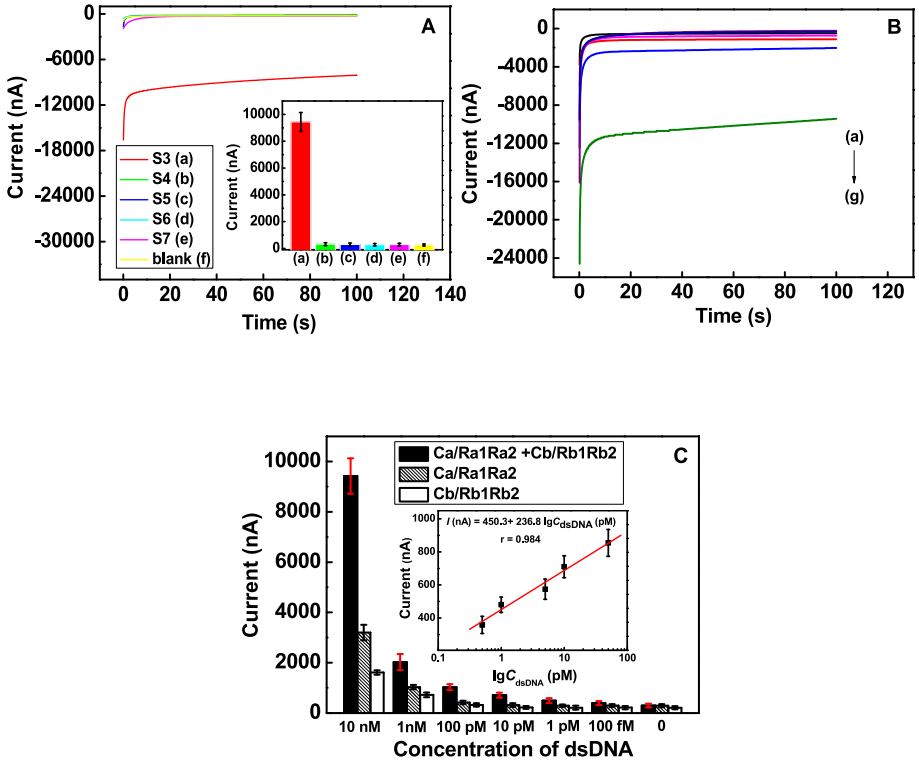

Fig. 3. (A) Current–time curves for the E-DNA biosensor based on dual-probe mode and enzyme-linked multiple signals amplification using d-AuE after hybridization with the complementary target dsDNA sequence S3 (a); with the five-base mismatch dsDNA sequence S4 (b); with the ten-base mismatch dsDNA sequence S5 (c); with PML sequence S6 (d); with RARα sequence S7 (e); and without any sequence (blank) (f). The inserted histogram shows the current signals of all targets at a concentration of 10 nM. (B) Current–time curves for the E-DNA biosensor based on the dual-probe mode and enzyme-linked multiple signals amplification using d-AuE after hybridization with the synthetic target dsDNA at a series of concentrations. (From (a) to (g): 0 pM, 100 fM, 1 pM, 10 pM, 100 pM, 1 nM, and 10 nM). (C) Comparison of the amperometric responses of the E-DNA biosensor using d-AuE modified with two groups of detection probes (Ca/Ra1Ra2+Cb/Rb1Rb2: black) or with a single group of detection probes (Ca/Ra1Ra2: dense or Cb/Rb1Rb2: white) after hybridization with the target dsDNA at different concentrations under the same condition. The inset shows a dose-response curve for the amperometric detection of the target dsDNA with concentrations from 0.50 pM to 50 pM. Error bars show the standard deviations of measurements taken from at least three independent experiments.

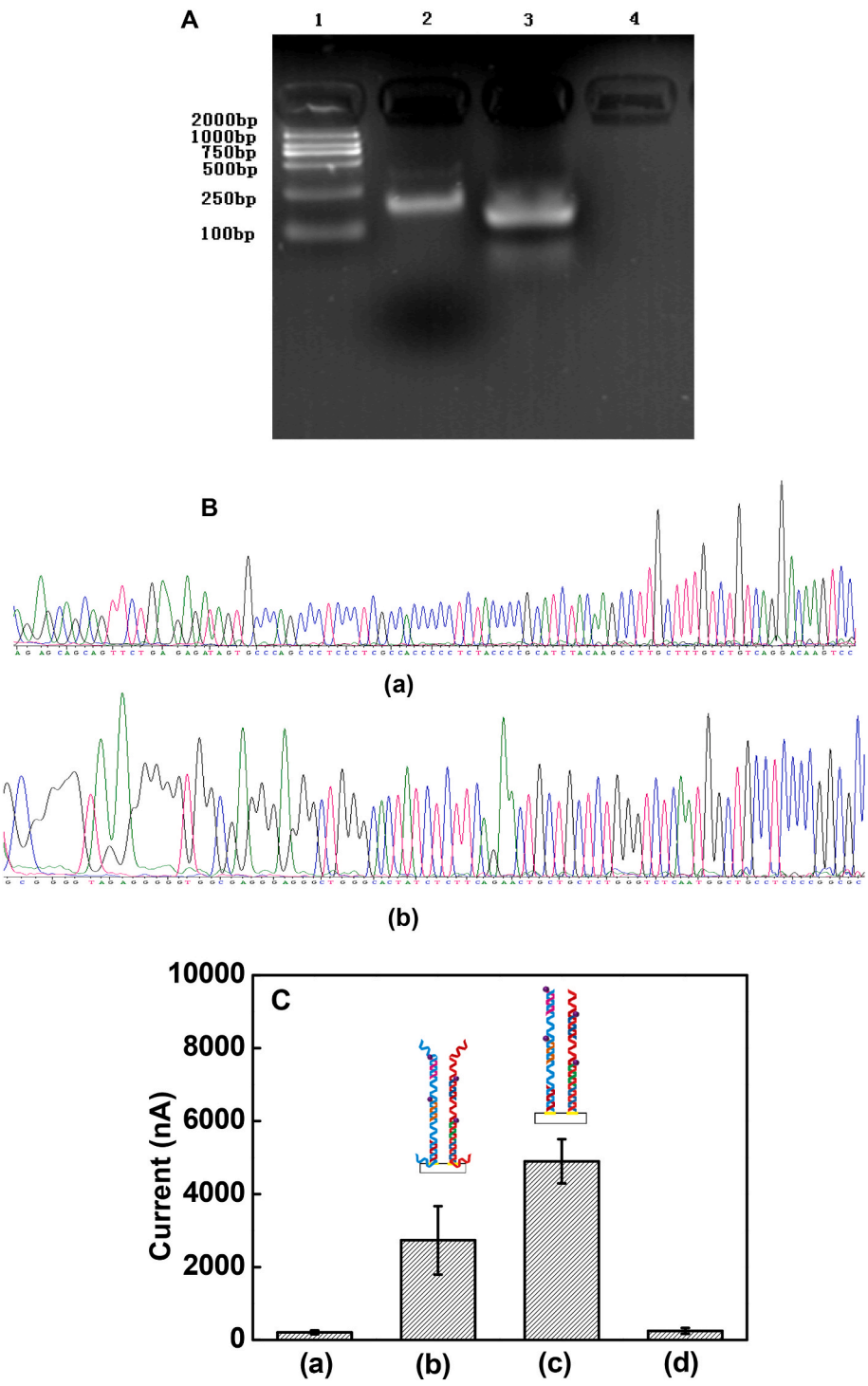

Fig. 4. (A) Electrophoretogram of the PCR-amplified products and enzyme-digested PCR products. The lanes from left to right: DL2000 DNA marker (lane 1, the brands from up to down: 2000 bp, 1000 bp, 750 bp, 500 bp, 250 bp, and 100 bp); positive PCR-amplified products (lane 2); enzyme-digested PCR products (lane 3); negative PCR-amplified products (lane 4). (B) The partial results for the gene sequencing of symmetric PCR products: (a) sequence 1, (b) sequence 2. (C) The bar graph of the current signals of the E-DNA biosensor based on the dual-probe mode and enzyme-linked multiple signals amplification using d-AuE after hybridizing with the blank (PCR system without cDNA template) (a), positive PCR-amplified products (151 bp) (b), enzyme-digested PCR products (122 bp) (c), and negative PCR-amplified products (d); all the real samples were presented at a concentration of 10 nM.

detect the PCR products and the enzyme-digested PCR products diluted by 100-fold to a final concentration of *ca.* 10 nM with *Tris*-HCl buffer (calculated according to the absorbance values measured at a wavelength of 260 nm). As displayed in Fig. 4C, the PCR products from the negative sample and background showed negligible current signals. Our biosensor could effectively detect the PCR products and the enzyme-digested PCR amplified products by producing more than an order of magnitude higher signal compared with the negative counterpart. Notably, compared with the enzyme-digested PCR product (122 bp), a 44% signal decrease was observed in the PCR products (155 bp) because of the possible steric effect caused by the large amplicon and the reduction of hybridization efficiency. This assay further demonstrated the applicability of the dual-probe E-DNA biosensor in real samples.

4. Conclusion

In summary, we have reported a simple and sensitive E-DNA biosensor for the dsDNA of the PML/RARα fusion gene by coupling dual-probe mode and enzyme-mediated multiple signal amplification. Compared to our previously reported dual-probe detection model, the proposed strategy displays significant advantageous features. First, it exhibits enhanced sensitivity and specificity for dsDNA determination,

even with large segments of the target dsDNA, beneficial from designing multiple reporter probes. Second, by the rational optimization of the complementary position of the capture probes and reporter probes, a high signal-to-noise ratio is achieved, although bountiful oligonucleotides (target dsDNA and six kinds of detection probes) exist in the same hybridization solution. Third, it does not need a complex analytical process (e.g. restriction endonuclease reaction) and the specialized modification of the detection probes; it requires a common single-channel potentiostat, which is adaptable for POCT device. Further, the practicability of the biosensor is proven to be comparably excellent in the PCR products and enzyme-digested PCR products of the PML/RARα fusion gene from the NB4 cell. Given all of these advantages, it furnishes an alternative approach for developing a rapid and sensitive diagnostic platform for various other diseases.

CRediT authorship contribution statement

Yun Lei: Investigation, Writing – original draft. **Kun Wang:** Investigation. **Jia-Yong Yang:** Investigation. **Xin-Hua Lin:** Project administration, Writing – review & editing. **Ai-Lin Liu:** Project administration, Supervision, Writing – review & editing.

Declaration of competing interest

The authors declare that they have no known competing financial interests or personal relationships that could have appeared to influence the work reported in this paper.

Data availability

No data was used for the research described in the article.

Acknowledgement

The authors gratefully acknowledge the financial support of the National Natural Science Foundation of China (22074017 and 82072379), Joint Funds for the Innovation of Science and Technology, Fujian Province (2019Y9005) and the Natural Science Foundation of Fujian Province, China (2019J01301).

Appendix A. Supplementary data

Supplementary data to this article can be found online at https://doi.org/10.1016/j.aca.2022.340436.

References

[1] M. Alcalay, D. Zangrilli, P.P. Pandolfi, L. Longo, A. Mencarelli, A. Glacomucci, M. Rocchl, A. Biondl, A. Rambaldi, F.L. Coco, D. Diverio, E. Donti, F. Grignani, P. G. Pelicci, Translocation breakpoint of acute promyelocytic leukemia lies within the retinoic acid receptor alpha locus, Proc. Natl. Acad. Sci. U.S.A. 88 (1991) 1977–1981.

[2] A.D. Goddard, J. Borrow, P.S. Freemont, E. Solomon, Characterization of a zinc finger gene disrupted by the t(15;17) in acute promyelocytic leukemia, Science 254 (1991) 1371–1374.

[3] R.P. Warrel Jr., H. de The, Z.Y. Wang, L. Degos, Acute promyelocytic leukemia, N. Engl. J. Med. 329 (1993) 177–189.

[4] F. Grignani, M. Fagioli, M. Alcalay, L. Longo, P.P. Pandolfi, E. Donti, A. Biondi, F. Lo Coco, P.G. Pelicci, Acute promyelocytic leukemia: from genetics to treatment, Blood 83 (1994) 10–25.

[5] M. Jeanne, V. Lallemand-Breitenbach, O. Ferhi, M. Koken, M. Le Bras, S. Duffort, L. Peres, C. Berthier, H. Soilihi, B. Raught, H. de Thé, PML/RARA oxidation and arsenic binding initiate the antileukemic response of As_2O_3, Cancer Cell 18 (2010) 88–98.

[6] Z.Y. Wang, Z. Chen, Acute promyelo-cytic leukemia: from highly fatal to highly curable, Blood 111 (2008) 2505–2515.

[7] L.-C. Francesco, C. Laura, B. Massimo, Laura Cicconi, Massimo Breccia, Current standard treatment of adult acute promyelocytic leukaemia, Br. J. Haematol. 172 (2016) 841–854.

[8] H. de The, P.P. Pandolfi, Z. Chen, Acute promyelocytic leukemia: a paradigm for oncoprotein-targeted cure, Cancer Cell 32 (2017) 552–560.

[9] G.S.G. Murthy, A. Szabo, L. Michaelis, K.S. Carlson, L. Runaas, S. Abedin, E. Atallah, Improving outcomes of acute promyelocytic leukemia in the current era: analysis of the SEER database, J. Natl. Compr. Cancer Netw. 18 (2020) 169–175.

[10] J. Kim, A.S. Campbell, B.E.F. de Avila, J. Wang, Wearable biosensors for healthcare monitoring, Nat. Biotechnol. 37 (2019) 389–406.

[11] L.C. Chen, E. Wang, C.S. Tai, Y.C. Chiu, C.W. Li, Y.R. Lin, T.H. Lee, C.W. Huang, J. C. Chen, W.L. Chen, Improving the reproducibility, accuracy, and stability of an electrochemical biosensor platform for point-of-care use, Biosens. Bioelectron. 155 (2020), 112111.

[12] Z.J. Zhang, R. Pandey, J.X. Li, J. Gu, D. White, H.D. Stacey, J.C. Ang, C. J. Steinberg, A. Capretta, C.D.M. Filipe, K. Mossman, C. Balion, M.S. Miller, B. J. Salena, D. Yamamura, L. Soleymani, J.D. Brennan, Y.F. Li, High-affinity dimeric aptamers enable the rapid electrochemical detection of wild-type and B.1.1.7 SARS-CoV-2 in unprocessed saliva, Angew. Chem.-Int. Edit. 60 (2021) 24266–24274.

[13] X.Y. Hua, J.J. Fan, L.Z. Yang, J. Wang, Y.Q. Wen, L. Su, X.J. Zhang, Rapid detection of miRNA via development of consecutive adenines (polyA)-based electrochemical biosensors, Biosens. Bioelectron. 198 (2022), 113830.

[14] M. Alafeef, K. Dighe, P. Moitra, D. Pan, Rapid, ultrasensitive, and quantitative detection of SARS-CoV-2 using antisense oligonucleotides directed electrochemical biosensor chip, ACS Nano 14 (2022) 17028–17045.

[15] D.W. Li, S. Ling, H.S. Wu, Z.Q. Yang, B. Lv, CRISPR/Cas12a-based biosensors for ultrasensitive tobramycin detection with single- and double-stranded DNA activators, Sens. Actuator B-Chem. 355 (2022), 131329.

[16] N. Wei, J.H. Chen, J. Zhang, K. Wang, X.W. Xu, J.H. Lin, G.W. Li, X.H. Lin, Y. Z. Chen, An electrochemical biosensor for detection of PML/RARα fusion gene using capture probe covalently immobilized onto poly-calcon carboxylic acid modified glassy carbon electrode, Talanta 78 (2009) 1227–1234.

[17] A.L. Liu, X.H. Chen, K. Wang, N. Wei, Z.L. Sun, X.H. Lin, Y.Z. Chen, M. Du, Electrochemical DNA biosensor based on aldehyde-agarose hydrogel modified glassy carbon electrode for detection of PML/RARα fusion gene, Sens. Actuators B-Chem. 160 (2011) 1458–1463.

[18] G.X. Zhong, A.L. Liu, X.H. Chen, K. Wang, Z.X. Lian, Q.C. Liu, Y.Z. Chen, M. Du, X. H. Lin, Electrochemical biosensor based on nanoporous gold electrode for detection of PML/RAR alpha fusion gene, Biosens. Bioelectron. 26 (2011) 3812–3817.

[19] L.M. Wang, L.Q. Lin, X.W. Xu, S.H. Weng, Y. Lei, A.L. Liu, Y.Z. Chen, X.H. Lin, Electrochemical biosensor for detection of PML/RARα fusion gene based on eriochrome cyanine R film modified glassy carbon electrode, Electrochim. Acta 69 (2012) 56–59.

[20] L.Q. Lin, Q.C. Liu, L.M. Wang, A.L. Liu, S.H. Weng, Y. Lei, W. Chen, X.H. Lin, Y. Z. Chen, Enzyme-amplified electrochemical biosensor for detection of PML-RARα fusion gene based on hairpin LNA probe, Biosens. Bioelectron. 28 (2011) 277–283.

[21] K. Wang, Z.L. Sun, M.J. Feng, A.L. Liu, S.U. Yang, Y.Z. Chen, X.H. Lin, Design of a sandwich-mode amperometric biosensor for detection of PML/RARα fusion gene using locked nucleic acids on gold electrode, Biosens. Bioelectron. 26 (2011) 2870–2876.

[22] Y. Lei, M.J. Feng, K. Wang, L.Q. Lin, Y.Z. Chen, X.H. Lin, Sequence-specific electrochemical detection of double-strand PCR amplicons of PML/RAR alpha fusion gene in acute promyelocytic leukemia, Anal. Bioanal. Chem. 405 (2013) 423–428.

[23] K. Wang, Y. Lei, Y.J. Zheng, Z.L. Sun, H.P. Peng, W. Chen, A.L. Liu, Y.Z. Chen, Dual-probe electrochemical DNA biosensor based on the "Y" junction structure and restriction endonuclease assisted cyclic enzymatic amplification for detection of double-strand DNA of PML/RARα related fusion gene, Biosens. Bioelectron. 71 (2015) 463–469.

[24] Y. Lei, K. Wang, S.Y. Wu, D.D. Huang, M. Dai, Y.J. Zheng, Z.L. Sun, Y.Z. Chen, X. H. Lin, A.L. Lin, 2′-Fluoro ribonucleic acid modified DNA dual-probe sensing strategy for enzyme-amplified electrochemical detection of double-strand DNA of PML/RARα related fusion gene, Biosens. Bioelectron. 112 (2018) 170–176.

[25] R.X. Shi, Z.G. Hu, H. Lu, L. Liu, L. Xu, Y.J. Liu, H.Z. Wu, B.S. Huang, G.J. Zhang, S. L. Chen, F. Yang, Hierarchical nanostructuring array enhances mid-hybridization for accurate herbal identification via ITS2 DNA barcode, Anal. Chem. 92 (2020) 2136–2144.

[26] K. Marchlewicz, I. Ostrowska, S. Oszwaldowski, A. Zasada, R. Ziolkowski, E. Malinowska, Molecular diagnostic of toxigenic *Corynebacterium diphtheriae* strain by DNA sensor potentially suitable for electrochemical point-of-care diagnostic, Talanta 227 (2021), 122161.

[27] Y. Liu, Y.D. Wei, Y.J. Cao, D.B. Zhu, W.G. Ma, Y. Yu, M.L. Guo, Ultrasensitive electrochemiluminescence detection of *Staphylococcus aureus via* enzyme-free branched DNA signal amplification probe, Biosens. Bioelectron. 117 (2018) 830–837.

[28] U.B. Gyllensten, M. Allen, Sequencing of *in vitro* amplified DNA, Methods Enzymol. 218 (1993) 3–16.

[29] F. Liu, H.X. Liu, Y.H. Liao, J.T. Wei, X.M. Zhou, D. Xing, Multiplex detection and genotyping of pathogenic bacteria on paper-based biosensor with a novel universal primer mediated asymmetric PCR, Biosens. Bioelectron. 74 (2015) 778–785.

[30] M. Zuker, Mfold web server for nucleic acid folding and hybridization prediction, Nucleic Acids Res. 31 (2003) 3406–3415.